ELSEVIER

Journal of Molecular Structure (Theochem) 584 (2002) 159–168

THEO CHEM

www.elsevier.com/locate/theochem

Propagator matrices as matrices of power's series. I. Its zeroth-order and the Pople–Santry model

C.A. Gómez, P.F. Provasi, G.A. Aucar*

Department of Physics, Northeastern University, Av. Libertad 5500, 3400 Corrientes, Argentina

Received 2 November 2001; accepted 10 December 2001

Abstract

The implementation and calculation of the principal propagator matrix elements as a power's series are presented. The scheme is applied to singlet- and triplet-type properties at random phase approach (RPA) level of approximation. Its application to both the polarizability and the J-NMR spectroscopic parameter by using localized molecular orbitals shows (i) any element of the principal propagator matrix can be expressed as a series, (ii) each series has a different rate of convergence which depends on the type of property analyzed, the model compound and the relative magnitude of the first element of that series, (iii) the Pople–Santry model is related with the first element of each series, (iv) convergence also depends on stability conditions, and (v) this scheme can easily be applied to ab initio post-RPA calculation of molecular properties.

Keywords: Principal propagator matrices; Pople–Santry model; Response molecular properties; Power series

1. Introduction

During the last few years, calculation of molecular properties within the algebraic approximation and using quite large basis sets are becoming more and more familiar because of improvement on hardware and also on algorithm efficiency [1–3]. Nevertheless, there are still some relevant computational bottlenecks. In the case of response methods, the inversion of the principal propagator matrix is one of them [4]. In order to overcome this problem, some alternative schemes were developed in which the inverse of that matrix is never calculated [5,6]. In such a case the physical information related with electronic molecular structure as a whole, which is contained within the principal propagator, is lost because that procedure modify in an incontrollable way the individual elements involved in the calculation. Then it deserves some relevant work to search for new procedures which maintain the inversion of the matrix calculation as such.

Some years ago, it was shown that the principal propagator matrix at random phase approach (RPA) level could be written as a power's series [7]. The first term of this series represents the crudest approach and is related only with the inverse of the differences between molecular orbital (MO) energies. A formal relationship between the development of the triplet principal propagator and the Pople–Santry (PS) model for NMR-J calculations was published recently [8]. A further step on that previous finding is presented here in two parts.

In part I, we shall show a generalization of the procedure outlined in Ref. [8]: Irrespective of the

* Corresponding author. Tel.: +54-3783-473931; fax: +54-3783-473930.

E-mail address: gaa@rec.unne.edu.ar (G.A. Aucar).

0166-1280/02/$ - see front matter
PII: S0166-1280(02)00015-5

spin dependence of the linear response property analyzed, the principal propagator matrix **P** can be expressed as power's series with an expansion parameter depending on the off-diagonal elements and inversely with the diagonal ones. It will be shown that each element of the **P** matrix can be approximated by a power's series and also that the rate of convergence is not the same for all elements. The number of terms necessary to get close results with respect to the final RPA values depends on the magnitude of the first element of each series and also on the type of property and the model compound analyzed.

In part II, we shall give an analysis of the calculation where non-singlet quasi-instabilities at RPA level of approach do arise. In such a case, the convergence is very slow for some particular terms of the principal propagator.

2. Theory

A general expression for calculating molecular properties within polarization propagator methods, at RPA level of approach, can be written as [4]:

$$R = \Omega \tilde{\mathbf{b}} \mathbf{P} \mathbf{b} \tag{1}$$

where Ω is a constant which contain the usual constant included in calculations. **P** which is called the principal propagator depends on the electronic molecular structure as a whole and also on the spin dependence of the property studied. Matrix **b** and its transpose $\tilde{\mathbf{b}}$ are called the property matrix.

The principal propagator matrix is built from the following elements

$${}^{m}\mathbf{P}^{-1}_{ia,jb} = ({}^{m}\mathbf{A} \pm {}^{m}\mathbf{B})^{-1}_{ia,jb} \tag{2}$$

where $m = 1(3)$ for singlet (triplet) type properties. When $m = 1(3)$ the $+(-)$ sign between ${}^{1}\mathbf{A}({}^{3}\mathbf{A})$ and ${}^{1}\mathbf{B}({}^{3}\mathbf{B})$ is applied. Matrix elements for **A** and **B** matrices are as follows [4]:

$$\begin{aligned} {}^{1}\mathbf{A}_{ia,jb} &= (\varepsilon_a - \varepsilon_i)\delta_{ab}\delta_{ji} + 2\langle aj|ib\rangle - \langle aj|bi\rangle \\ {}^{3}\mathbf{A}_{ia,jb} &= (\varepsilon_a - \varepsilon_i)\delta_{ab}\delta_{ji} - \langle aj|bi\rangle \\ {}^{1}\mathbf{B}_{ia,jb} &= \langle ab|ji\rangle - 2\langle ab|ij\rangle \qquad {}^{3}\mathbf{B}_{ia,jb} = \langle ab|ji\rangle \end{aligned} \tag{3}$$

The indices $i, j(a, b)$ account for bonding, non-bonding or antibonding (virtual) MOs; $\varepsilon_i(\varepsilon_a)$ represents their corresponding energies and the other elements are bi-electronic integrals. Singlet- or triplet-type property matrix elements are

$$\mathbf{b}_{ia} = \langle i|V|a\rangle \tag{4}$$

where V stands for the perturbation related with the property studied. For example, for the Fermi contact (FC) contribution to the J-NMR coupling, we have [4,9]

$$\mathbf{b}^{\mathrm{FC}}_{ia} = 4\pi \frac{\sqrt{2}}{3} g\beta\hbar\beta\gamma_N \langle i|\delta(r_i - R_N)|a\rangle \tag{5}$$

In the case of the static polarizabilities

$$\mathbf{b}^{\mathrm{pol}}_{ia} = (\vec{r})_{ia} \tag{6}$$

where $\vec{r}$ is the dipolar operator. The contribution from (localized/canonical) orbital within polarization propagator approach (C(L/C)OPPA) [10] scheme was developed to decompose the analysis of some properties in term of 'local' contributions, meaning the contribution from individual pathway terms which will be defined later.

The C(L/C)OPPA scheme assumes the monocentric approximation. When this method is applied on top of some semiempirical scheme, like MNDO [11], AM1 [12], INDO/S [13], etc. Eq. (1) can be expressed as:

$$R = \sum_{ia,jb} R_{ia,jb} = \Omega \sum_{ia,jb} b_{ia} P_{ia,jb} b_{jb} \tag{7}$$

Each $R_{ia,jb}$ corresponds to the contribution to the property R given by the 'coupling pathway' represented by virtual excitations $i \rightarrow a$, $j \rightarrow b$. We shall present results for two molecular properties, i.e. the FC term of indirect nuclear spin–spin couplings and static polarizabilities. Within the non-relativistic regime, the first of them is divided into four terms: Fermi contact (FC), spin–dipolar (SD), paramagnetic and diamagnetic spin–orbital (PSO and DSO). The last one is calculated as an average value from the reference wavefunction. The first three are given as [8]:

$$\begin{aligned} J_{NM} &= J^{\mathrm{FC}}_{NM} + J^{\mathrm{SD}}_{NM} + J^{\mathrm{PSO}}_{NM} = \sum_{\mathrm{X}_{ia,jb}} J^{\mathrm{X}}_{ia,jb} \\ &= \sum_{\mathrm{X}_{ia,jb}} \Omega^{\mathrm{X}} \mathbf{b}^{\mathrm{X}}_{ia,N} {}^{m}\mathbf{P}_{ia,jb} \mathbf{b}^{\mathrm{X}}_{ia,M} \end{aligned} \tag{8}$$

Each $J^{\mathrm{X}}_{ia,jb}$ is called an individual coupling pathway

contribution corresponding to X (FC, SD or PSO) nuclear spin–electron interaction mechanism. On the other hand, static polarizabilities are expressed as [14]:

$$\alpha = \sum_{ia,jb} \alpha_{ia,jb} = \sum_{ia,jb} d_{ia}\,{}^{1}\mathbf{P}_{ia,jb} d_{jb} \tag{9}$$

where

$$d_{ia} = \langle i|e\mathbf{r}|a\rangle \tag{10}$$

r being the electronic position vector.

3. The principal propagator matrix expressed as a matrix of power's series

The singlet ($^{1}\mathbf{P}$) or the triplet ($^{3}\mathbf{P}$) principal propagator matrix can be written as a matrix which consist of elements that are power's series, i.e. ${}^{m}\mathbf{P}_S$ [8]

$$({}^{m}\mathbf{P}_S)_{ia,jb} = [\mathbf{E}^{-1}(\mathbf{I} - {}^{m}\mathbf{N}\mathbf{E}^{-1})^{-1}]_{ia,jb} \tag{11}$$

$$({}^{m}\mathbf{P}_S)_{ia,jb} = \left(\mathbf{E}^{-1}\sum_{i=0}^{\infty}({}^{m}\mathbf{N}\mathbf{E}^{-1})^{i}\right)_{ia,jb} \tag{12}$$

$$({}^{m}\mathbf{P}_S)_{ia,jb} \approx \left(\mathbf{E}^{-1}\sum_{n=0}^{p}({}^{m}\mathbf{N}\mathbf{E}^{-1})^{n}\right)_{ia,jb} = ({}^{m}\mathbf{P}_S)_{ia,jb;p} \tag{13}$$

where p stands for the number of terms in each series corresponding to a given coupling pathway; **E** is the diagonal matrix when canonical MOs are used and is built from the difference of MO energies, and ${}^{m}\mathbf{N}$ represents the matrix of bi-electronic integrals present in Eq. (3). The power's series expansion for each element of ${}^{m}\mathbf{P}$ is allowed because of each element of the matrix **E** is larger than any of the elements of the ${}^{m}\mathbf{N}$ matrix [15,16].

It is easily seen that

$$\lim_{p\to\infty} {}^{m}\mathbf{P}_{S;p} \rightarrow {}^{m}\mathbf{P} \tag{14}$$

The ${}^{m}\mathbf{P}_S$ matrix can be written in terms of localized or canonical MOs. When the selected MOs are the canonical ones, the ${}^{m}\mathbf{E}$ is diagonal; otherwise it is non-diagonal. In such a case we should calculate a matrix where its diagonal elements are larger than the off-diagonal ones. Then it is possible to apply the same scheme as that used to calculate ${}^{m}\mathbf{P}_S$ within the canonical MO basis. We proceed by separating ${}^{m}\mathbf{E}$ in a diagonal plus a non-diagonal matrix

$${}^{m}\mathbf{E}_l = {}^{m}\mathbf{E}_{ld} + {}^{m}\mathbf{N}_l \tag{15}$$

and finally

$${}^{m}\mathbf{E}_l^{-1} \simeq {}^{m}\mathbf{E}_{ld}^{-1}\sum_{j=0}^{q}\left({}^{m}\mathbf{N}_l\,{}^{m}\mathbf{E}_{ld}^{-1}\right)^{j} \tag{16}$$

In this case, ${}^{m}\mathbf{E}_l^{-1}$ is calculated at the beginning of the process and then introduced in Eq. (13) for the calculation of each coupling pathway contribution. Given that the diagonal terms are much larger than the off-diagonal ones we can define the PS contribution as that obtained from ${}^{m}\mathbf{E}_l^{-1}$ in Eq. (16) with $j = 0$.

4. The Pople–Santry model

The simplest model proposed to analyze indirect nuclear spin couplings without resorting to an average energy scheme is the so-called PS [17]. At present, this is still the most common one used by experimentalist to interpret trends for indirect nuclear spin coupling constant [18,19]. Within this model, the FC term is written as:

$$J^{\mathrm{FC}}_{(N,M)} = -\left(\frac{44}{9}\right)\mu_\beta^2 h\gamma_N\gamma_M S_N^2(0)S_M^2(0)\Pi_{NM} \tag{17}$$

where β is the Bohr magneton, Π represents the mutual polarizability of MOs on nuclei N and M, and the other symbols are the gyromagnetic constant $\gamma_{N(M)}$ for nucleus $N(M)$. The mutual polarizability is

$$\Pi_{NM} = -4\sum_{i}^{\mathrm{occ}}\sum_{a}^{\mathrm{vac}} c_{iN}c_{aN}c_{iM}c_{aM}(\varepsilon_a - \varepsilon_i)^{-1} \tag{18}$$

where ε_a and ε_i are the orbital energies, i and a refer to canonical occupied and vacant MOs, respectively, $c_{i(a)N(M)}$ are the coefficients of the s-type AOs centred on the $N(M)$ atom. Each term of the mutual polarizability can be of either sign and refers to the contribution of each single excitation. This model includes all $i \rightarrow a$ single excitation.

Within the C(L/C)OPPA scheme implemented at MNDO [20], AM1 [21] or INDO/S [22] level of

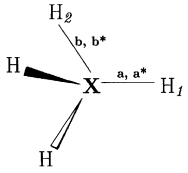

Fig. 1. Localized bonding orbitals a, b and antibonding orbitals a^*, b^* for the XH_4 molecule.

approach, the FC term has the expression

$$J^{\mathrm{FC}}(N,M) = \Omega^{\mathrm{FC}} S_N^2(0) S_M^2(0) \sum_{ia,jb} c_{iN} c_{aN} c_{jM} c_{bM}\, {}^3\mathbf{P}_{ia,jb}(E=0) \tag{19}$$

From this equation, it is straightforward to relate the PS model with the first term in the expansion by series of J^{FC}. That expansion of J^{FC} is

$$J_S^{\mathrm{FC}}(N,M) \approx \Omega^{\mathrm{FC}} S_N^2(0)_M^2(0) \times \sum_{ia,jb} c_{iN} c_{aN} c_{jM} c_{bM} \left(\mathbf{E}^{-1} \sum_{n=0}^{p} ({}^3\mathbf{N}\mathbf{E}^{-1})^n \right)_{ia,jb} \tag{20}$$

Each individual coupling pathway contribution is written then as a series

$$J_{S;ia,jb}^{\mathrm{FC}} = \Omega^{\mathrm{FC}} S_N^2(0) S_M^2(0) \times \Big[c_{iN} c_{aN} c_{jM} c_{bM} (\varepsilon_a - \varepsilon_i)^{-1} \delta_{ij} \delta_{ab} + c_{iN} c_{aN} c_{jM} c_{bM} \frac{(\langle ab|ji\rangle + \langle aj|bi\rangle)}{(\varepsilon_a - \varepsilon_i)(\varepsilon_b - \varepsilon_j)} + \text{higher order terms} \Big] \tag{21}$$

Here, the first term is the same as that of Eq. (17) representing the zeroth-order contribution within the polarization propagator scheme at any level of approach. In the same manner, it is possible to obtain zeroth-order contribution when PSO or SD terms are calculated with response schemes.

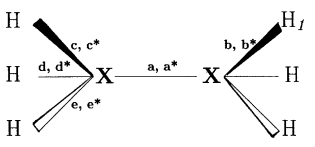

Fig. 2. Localized bonding orbitals a, b and antibonding orbitals a^*, b^* for the H_3XXH_3 molecule.

In the case of static polarizabilities, the series expansion can be written as [14]:

$$\alpha = \sum_{ia,jb} \alpha_{ia,jb} \tag{22}$$

where

$$\alpha_{ia,jb} = 4 \begin{cases} [r_{ia} r_{jb} + r_{jb} r_{ia}] P_{ia,jb} & \text{for } ia < jb \\ r_{ia} r_{ia} P_{ia,jb} & \text{for } ia = jb \end{cases} \tag{23}$$

5. Results and discussion

The geometry of all model compounds we have studied were optimized for consistency within the MNDO scheme. Given that the PS and our zeroth-order contribution are formally identical (within the C(L/C)OPPA scheme), we are interested in knowing how large is the PS contribution for one-bond and two-bond couplings in different model compounds. It is important to realize that within C(L/C)OPPA scheme, the atomic parameters like $S_N^2(0)$ are taken from ab initio calculations [20], i.e. they are not adjusted to experimental results as was the criteria used in the original PS version [17]. We applied our scheme of series to model compounds belonging to the series XH_4 and H_3XXH_3 with X = C, Sn and Pb. The analysis was done using localized MOs and their nomenclature is shown in Figs. 1 and 2. From now, we will name the indices with star as antibonding MOs and all others as bonding MOs. The coupling pathway bb^*bb^* means excitations from bonding to antibonding MOs belonging to the same bond. When the coupling pathway includes localized orbitals, which belong to bonds that do not contain both coupled nuclei we will indicate it with different letters depending on whether we are interested in a one-bond or two-bond coupling. When we consider two-bond couplings the main coupling pathway will contain four localized MOs: two (one occupied and one virtual) will connect the central atom with one of the coupled atoms; the other two will connect the central atom with the other coupled atom. In such a case, we will name that coupling pathway as aa^*bb^*.

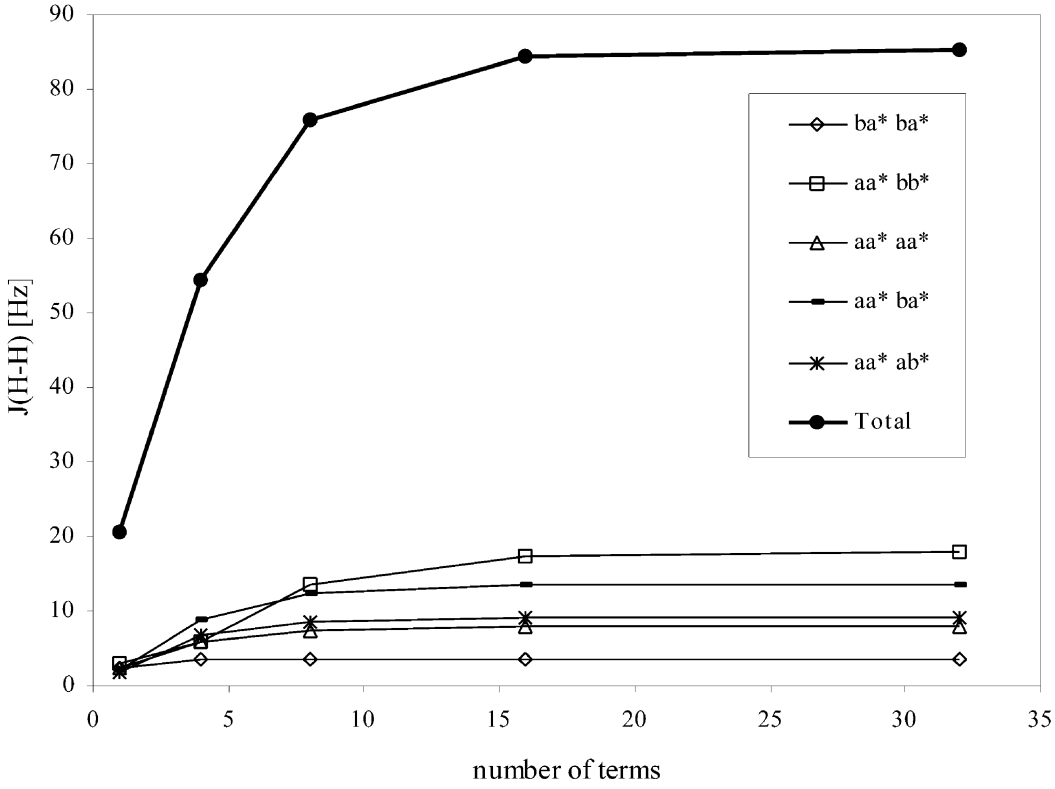

Fig. 3. $^{1}J_{Sn-H}$ coupling behaviour for different coupling pathways and its total value in SnH_4.

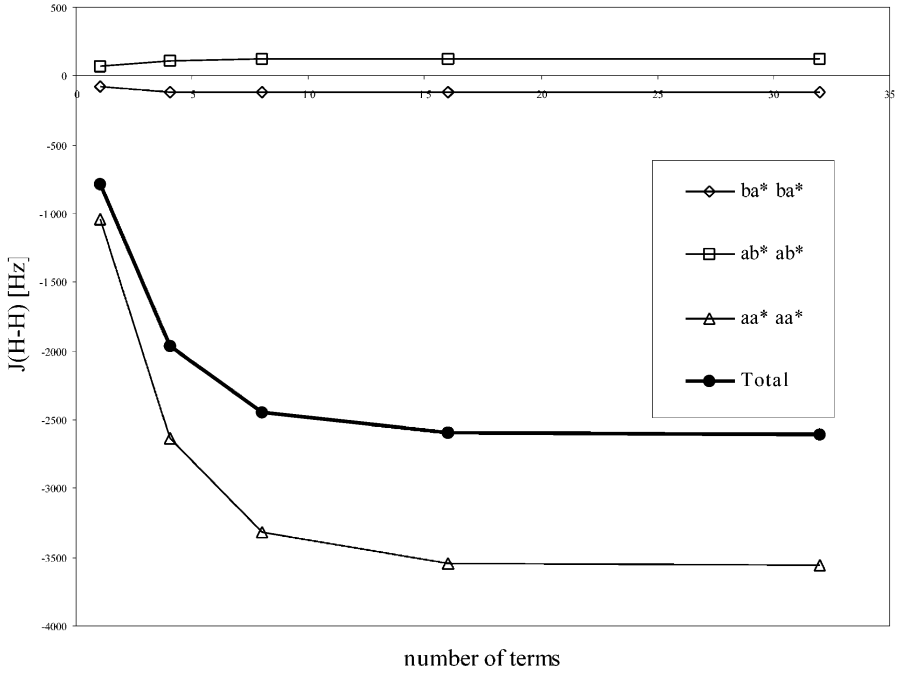

Fig. 4. $^{2}J_{H-H}$ coupling behaviour for different coupling pathways and its total value in SnH_4.

Table 1
$^{1}J^{FC}$ and $^{2}J^{FC}$ in PbH_4 and SnH_4 (nomenclature used is shown in Figs. 1 and 2)

Compounds	Coupling (Hz)	Coupling pathway	$n = 1$ (PS)	$n = 4$	$n = 8$	$n = 16$	$n = 32$	RPA	PS/RPA (%)
PbH_4	$^{2}J_{H_1-H_2}$	aa^*bb^*	3.10	12.96	37.08	51.93	53.63	54.12	5.74
		aa^*ba^*	3.62	15.33	22.36	25.10	25.36	25.34	14.29
		aa^*aa^*	5.21	13.17	17.14	18.52	18.64	18.64	27.95
		Total[a]	37.16	114.21	168.48	194.90	197.66	198.16	18.75
	$^{1}J_{Pb-H_1}$	ba^*ba^*	167.15	258.03	273.97	277.55	277.84	277.84	60.16
		ab^*ab^*	−166.77	−257.53	−273.46	−277.02	−277.31	−277.31	60.14
		aa^*aa^*	1531.68	3874.32	5040.70	5448.59	5482.55	5481.81	27.94
		aa^*bb^*	−10.72	−44.74	−128.01	−179.28	−185.13	−186.84	5.74
		ad^*aa^*	−381.96	−1003.51	−1152.55	−1220.91	−1228.70	−1224.65	31.19
		cd^*aa^*	−41.98	−203.87	−418.83	−511.58	−521.07	−511.36	8.21
		Total[a]	843.91	1735.39	2185.70	2279.61	2283.64	2287.97	36.88
SnH_4	$^{2}J_{H_1-H_2}$	aa^*bb^*	2.95	5.87	13.55	17.31	17.81	17.93	16.45
		aa^*ba^*	2.15	8.77	12.24	13.40	13.48	13.49	15.94
		aa^*ab^*	1.82	6.65	8.47	9.12	9.17	9.16	19.89
		aa^*aa^*	2.28	5.79	7.32	7.80	7.83	7.83	29.10
		Total[a]	20.06	54.46	75.96	84.37	85.20	85.32	23.51
	$^{1}J_{Sn-H_1}$	ba^*ba^*	−75.62	−113.54	−118.13	−118.95	−119.00	−119.01	63.54
		ab^*ab^*	76.94	115.49	120.13	120.96	121.02	121.02	63.58
		aa^*aa^*	−1035.00	−2631.14	−3323.50	−3541.58	−3557.07	−3557.94	29.10
		ac^*ac^*	120.51	258.83	292.06	306.52	307.62	307.26	39.22
		cc^*aa^*	14.99	74.50	123.91	139.46	140.77	141.06	10.63
		Total[a]	−779.92	−1970.42	−2452.03	−2592.78	−2601.32	−2601.48	29.98

[a] Total means the value of J computing all coupling pathways for each n.

Table 2
$^1J^{FC}$ in H_3PbPbH_3 and H_3SnSnH_3 (nomenclature used is shown in Figs. 1 and 2)

Compounds	Coupling (Hz)	Coupling pathway	$n = 1$ (PS)	$n = 5$	$n = 10$	RPA	PS/RPA (%)
H_3PbPbH_3	$^1J_{Pb-H_1}$	ce^*ce^*	−172.29	−199.22	−201.59	−202.03	85.28
		dc^*dc^*	519.59	636.66	658.35	664.23	78.22
		ee^*ee^*	−79.52	−142.66	−162.67	−168.21	47.27
		cc^*cc^*	1806.72	3154.64	3572.08	3685.97	49.02
		Total[a]	995.34	1526.68	1625.48	1632.46	60.97
	$^1J_{Pb-Pb}$	aa^*aa^*	6351.47	10 046.6	11 216.63	11 583.19	54.83
		ba^*ba^*	2275.67	2585.24	2647.84	2668.49	85.28
		ca^*ca^*	963.28	1063.51	1077.19	1081.49	89.07
		aa^*bb^*	−345.16	−1140.21	−1588.66	−1784.20	19.35
		aa^*cc^*	−155.70	−560.05	−819.09	−938.14	16.60
		Total[a]	831.59	2473.13	2851.58	2909.53	28.58
H_3SnSnH_3	$^1J_{Sn-H_1}$	ec^*ec^*	−257.31	−301.42	−306.58	−307.52	83.67
		cd^*cd^*	106.93	121.41	122.29	122.41	87.35
		cc^*cc^*	1339.88	−2234.42	−2457.96	−2501.13	53.57
		Total[a]	−1215.61	−2046.25	−2229.59	−2258.28	53.83
	$^1J_{Sn-Sn}$	aa^*aa^*	3837.78	6147.46	6724.16	6838.28	56.12
		ca^*ca^*	463.20	508.47	512.31	513.04	90.29
		ba^*ba^*	868.96	970.05	982.17	984.56	88.26
		ec^*ec^*	−128.62	−150.68	−153.25	−153.72	83.67
		Total[a]	1954.07	3799.99	4217.16	4271.49	45.75

[a] Total means the value of J computing all coupling pathways for each n.

5.1. One-bond couplings

In Figs. 3 and 4, the different rate of convergence for some selected coupling pathways of the FC term in X–H and H–H of XH_4 (X = Sn and Pb) is shown (Table 1). The same patterns are observed for X = C and Si. The main coupling pathway, i.e. aa^*aa^*, has a PS term which represents 32.75% for Sn and 27.95% for Pb with respect to their corresponding total RPA values. These terms got values which are less than 0.6% of error after 16 iterations. They also give, by far, the most important contribution to the total coupling following a close relation with that. There are some other terms with a PS value that have a larger percentage and a quicker convergence like the ones called ab^*ab^* and ba^*ba^*. There are some others which have a much smaller percentage between its PS and RPA values like aa^*bb^*. This term has a PS/RPA relation of 5.74% for X = Pb. Its rate of convergence is much slower than that of the principal terms.

When comparing the different rate of convergences for coupling pathways of ^1J(Pb–Pb) in the model compound H_3PbPbH_3, it is evident that the pattern found for XH couplings is even more pronounced (Table 2). The principal coupling pathway, aa^*aa^*, starts with a PS value that is 54.83% of its RPA value. After 10 iterations, this coupling pathway reaches a value which is less than 3% difference with respect to its RPA. The coupling pathways called aa^*cc^* or aa^*bb^* start with a PS/RPA percentage of 16.60 or 19.35% and after 10 iterations they reach a value which is within 10% of its final RPA. A similar pattern shows the X–X couplings for other H_3XXH_3 model compounds (X = C, Si and Sn), though the behaviour is less pronounced. In the case of X = C, the PS/RPA percentage for the main coupling pathway is 64.70% and after 10 iterations, it reaches a value which is less than 0.6% of its RPA value.

5.2. Two-bond H–H couplings

For two-bond H–H couplings, the rate of convergence for some of the main coupling pathways follows a different pattern. The principal coupling

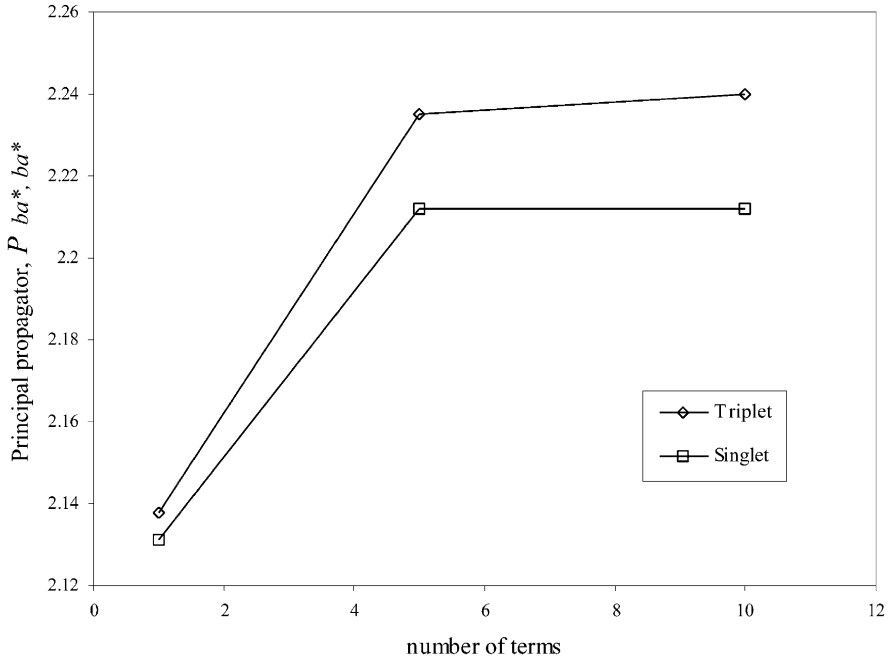

Fig. 5. Triplet and singlet terms for the coupling pathway a, a^* a, a^* in H_3PbPbH_3.

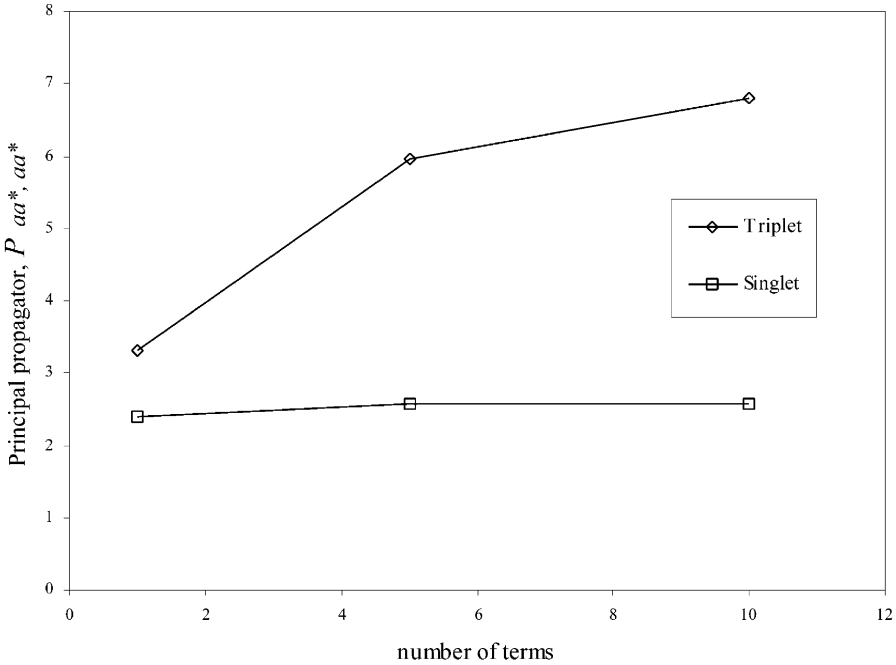

Fig. 6. Triplet and singlet terms for the coupling pathway a, b^* a, b^* in H_3SnSnH_3.

pathway, i.e. aa^*bb^*, has a value which represents 16.51% for X = Sn and 5.73% for X = Pb with respect to their corresponding RPA values. Convergence is reached after 32 iterations. Again the PS contribution for other coupling pathways varies between 29 and 63% in the case of X = Sn and from 14 to 60% when X = Pb. The geminal coupling pathways have a slower rate of convergency compared with one-bond coupling pathways. This behaviour becomes more pronounced when X goes down in the periodic table. It also depends on the model compounds analyzed, i.e. when comparing similar coupling pathways in CH_2O or XH_4, the rate of convergence is quite different from one and other.

5.3. Triplet- vs singlet-type series

Triplet- or singlet-type principal propagators have different parameters within each series expansion as shown in Eqs. (11)–(13). Then we could ask for their relative rate of convergency. We will concentrate on two coupling pathways in order to show the different behaviours which depends on the spin dependence of the propagators.

In Figs. 5 and 6, the convergence of the same aa^*aa^* and ab^*ab^* coupling pathways are shown for triplet- and singlet-type propagators. Singlet needs less than 10 terms in series expansion but its triplet counterparts needs more than 10 terms to get the convergence. The PS value for any singlet-type series is large compared with its RPA total value. This is not the case for triplet-type series. This behaviour is related with the stability problem and will be treated in extense in part II. In the case of X = Pb, it is seen that the principal propagator of the main coupling pathway gets a value that is more than twice its value for X = Sn. This indicates a quasi-instability for that calculation [23].

6. Concluding remarks

In this paper, we present for the first time the numerical results from a new scheme which allow us to calculate in an explicit way the principal propagator matrix in such a way that its physical content is preserved. The efficiency of that scheme is good enough to propose it as a good candidate to be applied on any ab initio code. Work on these lines are on the way in our Laboratory.

From the analysis presented in Section 2, it is shown that *each* coupling pathway could be written as a power series where its first term is related with the PS model. For each coupling pathway, this first term has different percentage of its RPA total value. It could have a value which fluctuates from approximately 6 to 60% depending on the coupling studied and also on the model compound. There are also different rate of convergence for each series belonging to a different coupling pathways.

It is also a remarkable fact that each coupling pathway has a different behaviour depending on the spin dependence of the property studied. The singlet-type properties have a much better and fast convergence. In the case of triplet-type molecular properties, like J^{FC}, that convergence depends on the particular coupling pathway and also on the model compound. As shown in Fig. 5, the pathway aa^*aa^* has a fast convergency for a singlet-type property but a very slow convergency for a triplet-type property. This behaviour is more pronounced in the case of X = Pb compared with X = Sn for H_3XXH_3 model compounds.

References

[1] T. Helgaker, M. Jaszunski, K. Ruud, Chem. Rev. 99 (1999) 293.
[2] P.F. Provasi, G.A. Aucar, S.P.A. Sauer, J. Chem. Phys. 115 (2001) 1324.
[3] P.F. Provasi, G.A. Aucar, S.P.A. Sauer, J. Chem. Phys. 112 (2000) 6201.
[4] J. Oddershede, P. Jorgensen, D.L. Yager, Comput. Phys. Rep. 2 (1984) 33.
[5] J. Olsen, P. Jorgensen, J. Chem. Phys. 82 (1985) 3235.
[6] M.J. Packer, E.K. Dalskov, T. Enevoldsen, H.J.Aa. Jensen, J. Oddershede, J. Chem. Phys. 105 (1996) 5889.
[7] G.A. Aucar, PhD Thesis, University of Buenos Aires, 1991.
[8] R.H. Contreras, M.C. Ruíz de Azúa, C.G. Giribet, G.A. Aucar, R. Lobayan de Bonczok, J. Molec. Struct. (Theochem) 249 (1993) 284.
[9] N.F. Ramsey, Phys. Rev. 91 (1953) 303.
[10] A.C. Diz, C.G. Giribet, M.C. Ruíz de Azúa, R.H. Contreras, Int. J. Quant. Chem. 663 (1990) 37.
[11] M.J.S. Dewar, W. Thiel, J. Am. Chem. Soc. 99 (1981) 4899.
[12] M.J.S. Dewar, E.G. Zoebisch, E.F. Healy, J.J.P. Stewart, J. Am. Chem. Soc. 3902 (1985) 107.
[13] M.C. Zerner, G.H. Loew, R.F. Kirchner, U.T. Mueller-Westerhoff, J. Am. Chem. Soc. 589 (1980) 102.

[14] C.G. Giribet, M.D. Demarco, M.C. Ruíz de Azúa, R.H. Contreras, Mol. Phys. 91 (1997) 105.
[15] P.O. Löwdin, J. Math. Phys. 3 (1962) 969.
[16] P.O. Löwdin, Phys. Rev. 139 (1965) 357.
[17] J.A. Pople, D.P. Santry, Mol. Phys. 8 (1964) 1.
[18] J. Mason (Ed.), Multinuclear NMR Plenum Press, New York, 1987 Chapter 4.
[19] J. Kowalewski, Progress in NMR Spectroscopy, vol. 32, Pergamon Press, New York, 1977 p. 11.
[20] G.A. Aucar, R.H. Contreras, J. Magn. Reson. 93 (1991) 413.
[21] G.A. Aucar, E. Botek, S. Gomez, E. Sproviero, R.H. Contreras, Organomet. Chem. 524 (1996) 1.
[22] E. Botek, G.A. Aucar, M. Cory, M. Zerner, J. Organomet. Chem. 598 (2000) 193.
[23] R.M. Lobayan, G.A. Aucar, J. Mol. Struct. (Theochem) 452 (1998) 13.